The Wind-wave Tank of the University of Hamburg

Martin Gade

Universität Hamburg, Institut für Meereskunde
Troplowitzstraße 7, 22529 Hamburg, Germany
Tel.: +49 40 42838 5450; Fax: +49 40 42838 5713;
E-mail: gade@ifm.uni-hamburg.de

Description of the facility

The wind wave tank facility of the University of Hamburg is located in a hall at the Hamburg Department of the Federal Waterways Engineering and Research Institute in Hamburg-Rissen. The tank is 26 m long and 1 m wide. It is filled with freshwater and has a mean water depth of 0.5 m. The wind tunnel height is 1 m, and the effective (maximum) fetch is 19 m. Measurements are usually being performed at fetches between 12.5 m and 15.5 m. A radial blower provides wind speeds between 1.5 m/s and 25 m/s, while mechanical waves with frequencies between 0.7 Hz and 2.5 Hz can be generated with a hydraulic wave flap. In addition, mechanical waves with frequencies higher than 2.5 Hz may be generated using a wave follower that has been converted to a wave generator by attaching a Styrofoam paddle and driving it with a sinusoidal power input.

Fig. 1: photograph of the wind-wave tank of the University of Hamburg

A beach for the efficient damping of the surface waves is located at the leeward end of the tank (see Fig. 2). In the measurement area the metallic roof plates have been replaced by Styrofoam panels to ensure the transmission of microwaves. Plates of microwave absorbing material have been fixed upon the Styrofoam panels in the direction of the specular reflected radar beams (see Fig. 2). A background current causing a minimal overflow at the beach is being maintained with a permanent water inflow at the windward end of the tank. For more detailed information about the wind wave tank see Hühnerfuss et al. (1976).

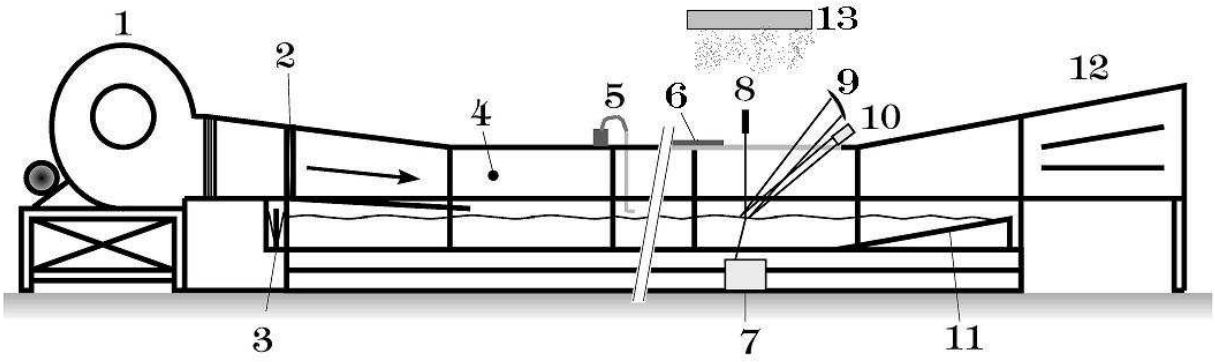

Fig. 2: schematic of the wind-wave tank of the University of Hamburg.
1: radial blower; 2: honeycomb; 3: wave flap; 4: anemometer; 5: pump; 6: Styrofoam panels with absorber material; 7: slope-gauge optics; 8: laser; 9: X band antennae; 10 additional microwave sensors (Ka band or W band) or video camera; 11: beach; 12: diffusor; 13: rain generator.

In order to simulate reliably the morphological structure of natural sea slicks, monomolecular surface films can be produced by distributing surface-active substances (e.g., oleyl alcohol, palmitic acid methyl ester, or triolein) on the water surface with the help of the spreading solvents ethanol or toluol. Usually, the 75 mMol/L solution is deployed at 5.5 m – 7.5 m fetches using a pipette that is fixed such that the drops fall from a height of a few millimeters without plunging deeply below the water surface. This allows for the optimum spreading of the monolayer without significant losses to the bulk water. The films are transported by the waves, the wind, or the background current towards the leeward end of the tank.

More recently, a rain generator has been added to the tank facility, in order to allow for dedicated experiments on the action of impinging rain drops on the upper water layer and, in particular, on the wind-induced wave field. The rain generator consists of six interconnected tubs (each 0.8 m long, 0.6 m wide, and 0.3 m high) that are mounted in an aluminum frame at a height of 4.5 m above the mean water surface. Approximately 3000 hypodermic needles are inserted into the bottoms of the tubs in a triangular pattern with a needle separation of 30 mm. With this set-up the total area agitated by rain is 2.3 m^2, reaching from 11,5 m to 13.8 m fetch. The diameter of the rain drops is 2.9 mm and they attain an impact velocity of 8.1 m/s, which is about 85% of their terminal velocity. Currently, high rain rates of 160, 210, and 300 mm/h are produced by the rain generator. Fig. 4 shows a photograph of the rain generator seen from below.

X-band radar measurements are performed with two upwind-looking radar antennae for transmission and reception using a coherent continuous wave (CW) 9.8 GHz (X band) scatterometer that operates at an incidence angle between 20° and 55°. The X band microwave beam is focused on the water surface by means of a bistatic parabolic reflector construction mounted on a metal frame that is fixed to the roof beams of the hall where the wind wave tank is located. Temporarily, a CW 37 GHz (Ka band) scatterometer of the

Russian Academy of Sciences operating at an incidence angle of 53° was used whose microwave beam was focused on the water surface using a plastic lens. Recently, a frequency-modulated (FM) CW radar working at 94 GHz (W band) was added to the instrumental set-up. The chirp bandwidth of the system is 3 GHz and, therefore, the range resolution is approx. 5 cm, thus allowing for high-resolution studies of the generation and propagation of small-scale roughness on the water surface.

Fig. 3: photograph from inside the wind-wave tank. The quadratic windows at the tank's bottom are used for the laser wave-slope measurements.

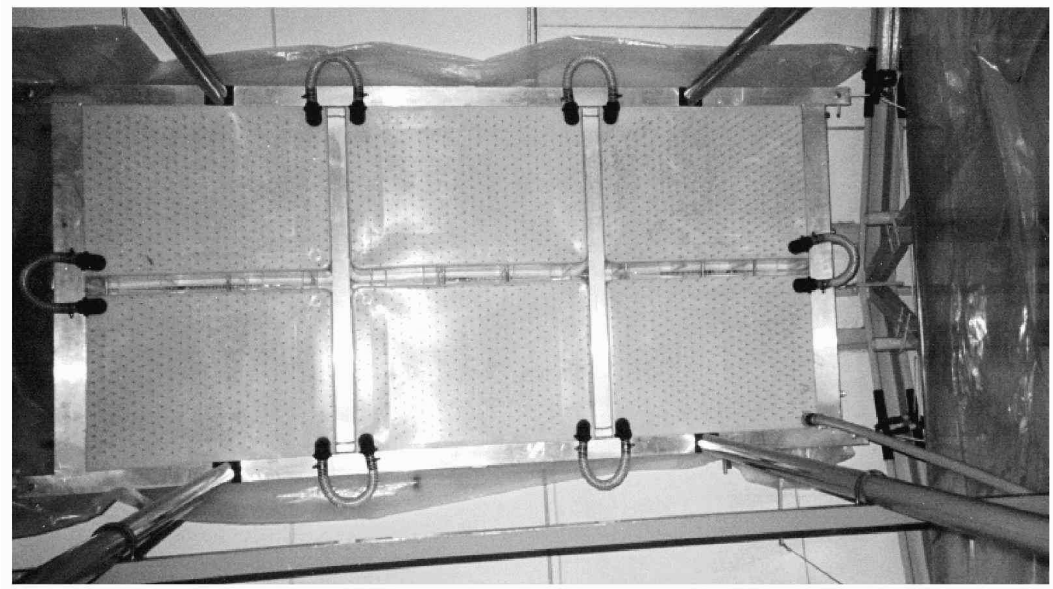

Fig. 4: photograph of the rain generator seen from below.

The reference wind speed is measured at the wind entrance 65 cm above the mean water surface level using a propeller-type anemometer. Wave heights are measured using a resistant-type wire wave gauge (Lobemeier, 1981) with a 0.075 mm diameter tungsten wire whose penetration point into the water is located at a distance of 22 cm laterally from to the radar footprints (i.e., at the same fetch length). Wave slopes are measured using a narrow-beam laser slope gauge (Lange et al., 1982) whose footprint is in the center of the radar footprints. The frequency resolutions of the sensors are about 30 Hz and better than 200 Hz, respectively. Two video cameras allow for optical measurements (up to 1000 × 1000 pixels) at high imaging rates of up to 120 Hz.

Fig. 5: photograph showing the upwind-looking W-band radar during a measurement with wind waves.

Measurements of wave damping by monomolecular surface films (Hühnerfuss, 1986; Lange and Hühnerfuss, 1978, 1984; Gade et al., 1998a)

Measurements of the damping of small gravity and gravity-capillary water surface waves covered with monomolecular organic films of different visco-elastic properties were performed in the wind wave tank facility of the University of Hamburg. The wind speed dependence of the radar cross sections for X and Ka band was measured with upwind looking microwave antennas. It was shown that Marangoni damping theory (Alpers and Hühnerfuss, 1989), which describes the damping of water surface waves by visco-elastic surface films, is not the only damping mechanism in wind wave tank experiments where the wind sea is not fully developed. The other source terms of the action balance equation, i.e., the energy input to the water waves from the wind, the nonlinear wave-wave interaction, and the dissipation by wave breaking are affected differently by the various substances. This is caused by the different visco-elastic properties of the substances, i.e., by the different intermolecular

interactions of the film molecules. A slight dip in the wind dependence of the radar cross section at Ka band at wind speeds of 8–9 m/s was measured which corresponds to comparable reductions of the mean squared wave height and wave slope. Higher polarization ratios (i.e., the ratios of the radar backscatter at vertical and horizontal polarization) than predicted by simple Bragg scattering theory for X band at low wind speeds and different incidence angles were explained within a (three-scale) composite-surface model. At higher wind speeds, where the polarization ratio decreases rapidly, breaking by wedges and spilling breakers was hypothesized to become more dominant. The dependence of the polarization ratio on the coverage of the water surface with a slick was explained qualitatively by means of the composite-surface model. Finally, it was stated that wind wave tank measurements in the presence of monomolecular surface films are very useful for the verification of theories concerning radar backscattering, wave damping, wind-wave and wave-wave interactions.

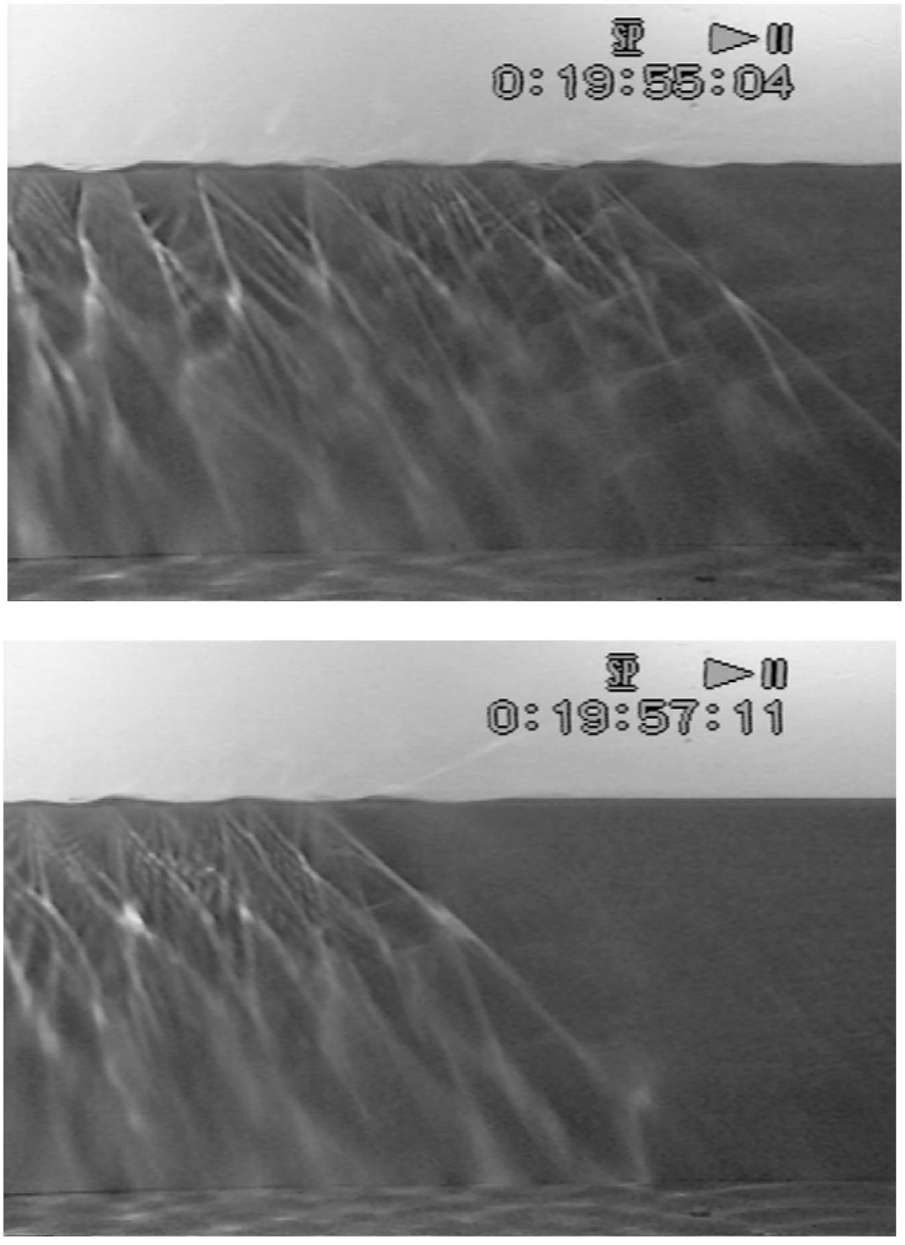

Fig. 6: series of video images (side-view into the wind-wave tank) showing the wave-damping effect of a monomolecular surface film consisting of oleyl alcohol. Upper image: wind waves (5 m/s) refracting the light; lower image: arrival of slick damping the waves (right image half)

Measurements of bound gravity-capillary waves (Gade et al., 1998b)

Measurements of the surface elevation and surface slope and of the backscattered radar power at X and Ka band were carried out in a wind wave tank with mechanically generated gravity waves as well as with wind-generated waves on slick-free and slick-covered water surfaces. The aim of this investigation was to obtain further insights into the characteristics of short gravity-capillary waves responsible for the X and Ka band backscattering, when the water surface is slick-free or covered with a monomolecular slick consisting of oleyl alcohol. Measurements of the radar Doppler shifts show that, on a slick-free water surface, bound gravity-capillary (X and Ka band Bragg) waves are generated at the crests of steep gravity waves with frequencies between 3 Hz and 5 Hz. Steep 2 Hz waves do not generate bound Ka band Bragg waves, thus, the Ka band backscatter is then associated with the breaking of the steep 2 Hz waves. For X band, the backscatter is caused by both bound harmonics and wave breaking. In the whole wind speed range used in the present investigation (1.5 m/s to 10 m/s), bound gravity-capillary waves contribute to the X and Ka band backscatter from a slick-free water surface, whereas their fraction on the Bragg waves depends on radar band and wind speed. Furthermore, it is shown that the coverage of the water surface with a monomolecular surface film has a strong influence on the generation of bound waves at the crests of the gravity waves. Whereas a mixture of bound and freely propagating Bragg waves is responsible for the radar backscattering at X and Ka band at wind speeds below 7 m/s, the strong damping of the gravity waves by the slick at wind speeds of approx. 8 m/s leads to the disappearance of the bound Bragg waves. Thus, a reduction of the measured Doppler shifts, both at X and Ka band, to values corresponding to freely propagating Bragg waves was observed. Moreover, an increase of the measured X and Ka band damping ratios (the ratios of the radar backscatter from a slick-free and a slick-covered water surface) in that particular wind speed range was measured, which can also be related to the disappearance of the bound Bragg waves. It was concluded that the obtained results are important for the interpretation of former results of radar backscattering measurements with oceanic surface films.

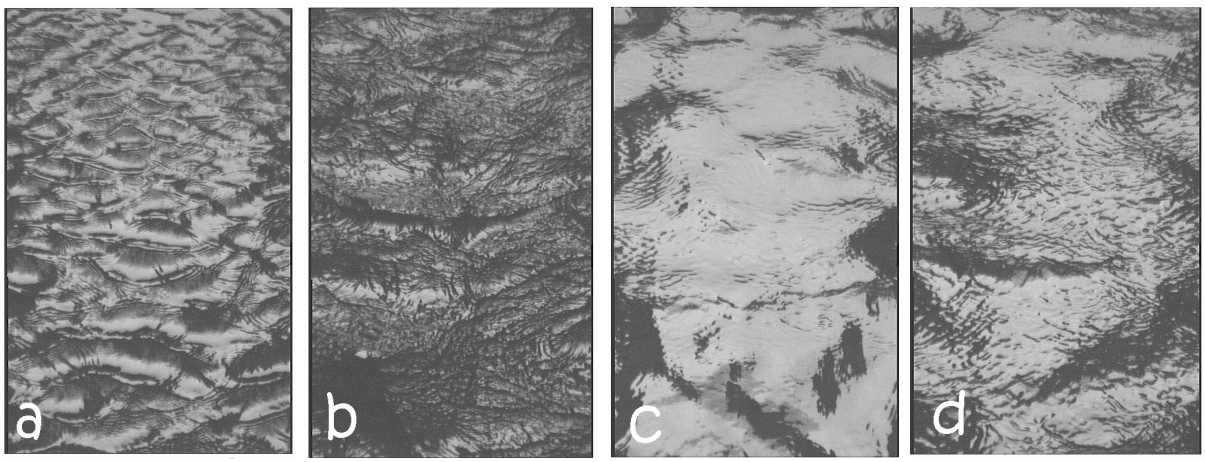

Fig. 7: video images of bound and free wind waves; a: 5 m/s, slick-free; b: 9 m/s, slick-free; c: 9 m/s, oleyl alcohol slick; d: 9 m/s, palmitic acid methyl ester slick

Measurements with artificial rain (Lange et al., 2000; Braun et al., 2002)

On the ocean, rain-induced turbulence results in a relatively thin "mixed layer" which is very important for heat and gas exchange processes at the air-sea interface. This rain-induced turbulence is intimately related to the rain splash products, which strongly affect radar remote sensing signals. Particle Image Velocimetry (PIV) and Particle Tracking Velocimetry (PTV) techniques have been used in experimental tanks to investigate the subsurface turbulence caused by raindrops impinging on a water surface (Fig. 9) with and without the effect of wind. We applied a photographic technique in a wind-wave tank with a large rain area (2.3 m^2) by using two different colored photographic flashes, oriented to illuminate the same area of interest. The flashes were fired with a preset time delay to produce a double exposure on a single color film frame. Standard correlation processing of the converted-to-grayscale image provided scalar information. In addition, digital PIV experiments using a dual ND-YAG laser were done in a small glass tank using single and multiple rain drops. The scale of the turbulence and the thickness of the rain-induced "mixed layer" were measured to be up to 15 cm, depending on rain rate. They were compared to acoustic doppler velocimeter (ADV) and dye studies. Using our results we were able to better interpret results of the analyses of synthetic aperture radar (SAR) images and of former radar backscattering measurements performed under the same laboratory conditions.

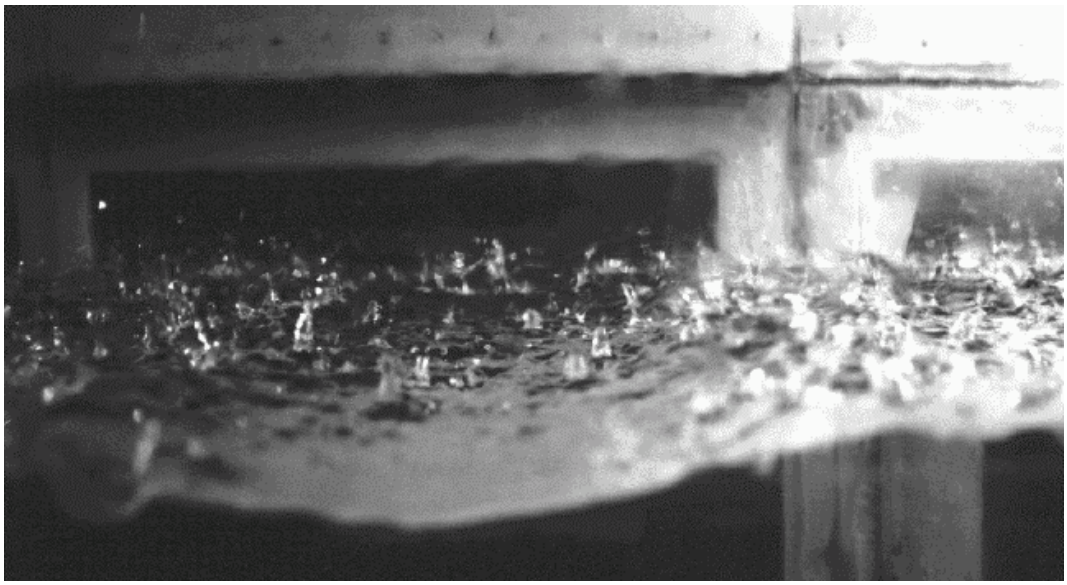

Fig. 8: photograph of splash products of heavy rain impinging on wind-induced waves

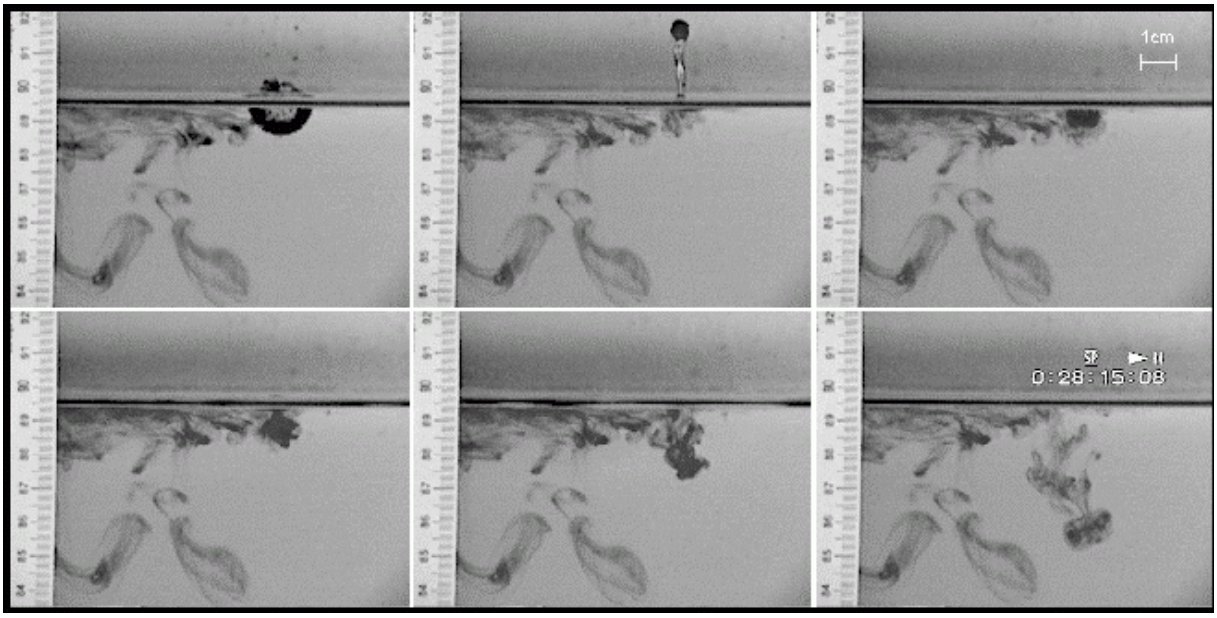

Fig. 9: series of video images taken while a dyed rain drop was impinging on a (flat) water surface. Note the generation of the cavity (top left) and of the stalk (top middle), and the impinging of the secondary drop (top right) that produces sub-surface turbulence (bottom row). Static features were caused by former rain drops.

Further wind-wave tank measurements using wave-height and wave-slope gauges and a coherent 9.8~GHz (X band) scatterometer were carried out when the water surface was agitated by heavy rain (160 mm/h to 300 mm/h) and by wind (2 m/s to 12 m/s). The upwind-looking scatterometer was operating at co- (VV- and HH) and cross- (HV-) polarization at a steep incidence angle of 28°. In the presence of rain the power spectral density of the wind-wave spectra is enhanced at frequencies above about 5 Hz and it is reduced at lower frequencies. This is the net effect of enhancement of the surface roughness by the rain-induced splash products and of wave damping by the rain-induced turbulence. The wave spectrum is isotropic in the presence of rain and without wind or at low wind speed, and it becomes anisotropic with increasing wind speed. We measured isotropic (rain-dominated) wave spectra at low wind speeds and anisotropic (wind-dominated) wave spectra at high wind speeds, with a transition wind speed increasing with increasing rain rate. The radar backscattering at co-polarization at low wind speeds is mainly caused by the rain-induced ring waves, whereas at cross-polarization at all wind speeds other rain-induced splash products, like crowns, stalks, and cavities, are the dominant scatterers. We found a rain-induced increase of the radar backscatter at co-polarization up to 9 m/s and at cross-polarization at all wind speeds. At cross-polarization the radar backscatter slightly depends on rain rate. Using our results an improved analysis of spaceborne synthetic aperture radar (SAR) images of tropical rain cells was performed. The results of this investigation will help to explain observations of rain events over the ocean with multi-frequency synthetic aperture radar and can improve radar backscatter models of the rain- and wind-roughened water surface.

Measurements at the edges of monomolecular slicks (Gade et al., 2002)

In order to provide data for training automated image analysis algorithms we have carried out laboratory measurements in the wind-wave tank of the University of Hamburg. One goal was to investigate the small-scale roughness of the water surface at the edges of quasi-biogenic

monomolecular surface films consisting of oleyl alcohol, triolein, and palmitic acid methyl ester. At wind speeds between 3 m/s and 9 m/s, at a fetch of 7.5 m small amounts of these substances were carefully deployed on the water surface, thus allowing for wave measurements at either end (i.e. downwind and upwind) of the surface films. A video camera and a 10 GHz (X-band) scatterometer were both looking upwind at the same spot on the water surface. In parallel, we used a two-dimensional laser slope gauge to measure the wave slope in the center of the camera's and scatterometer's footprint. The downwind edge of surface films usually is sharp, whereas the upwind edge is tattered and diffuse (see Fig. 10). However, we found that this effect depends on both the deployed substance and on the wind speed. Apart from the fact that the waves are propagating into the slick on its windward side, one must take into consideration that the damping capability of the slick material may be different at the downwind and upwind edges of the surface film, due to different states of film compression in these areas. Therefore, the observed effects depend on the visco-elastic properties of the deployed substance, which in turn may vary with wind speed. We also found that the spectral density of small-scale waves, which are bound to the dominant wind waves, in some cases strongly varies while the slick is drifting apart. This effect was shown and interpreted qualitatively using the video data, and quantitatively using the scatterometer and laser gauge data. There is evidence that the reflection of sunlight predominantly depends on the spectral density of free waves, whereas the bound waves strongly influence the radar backscattering at X-band. Therefore, our results are important for a better interpretation of field data that contributes to an improvement in the detection of marine surface slicks.

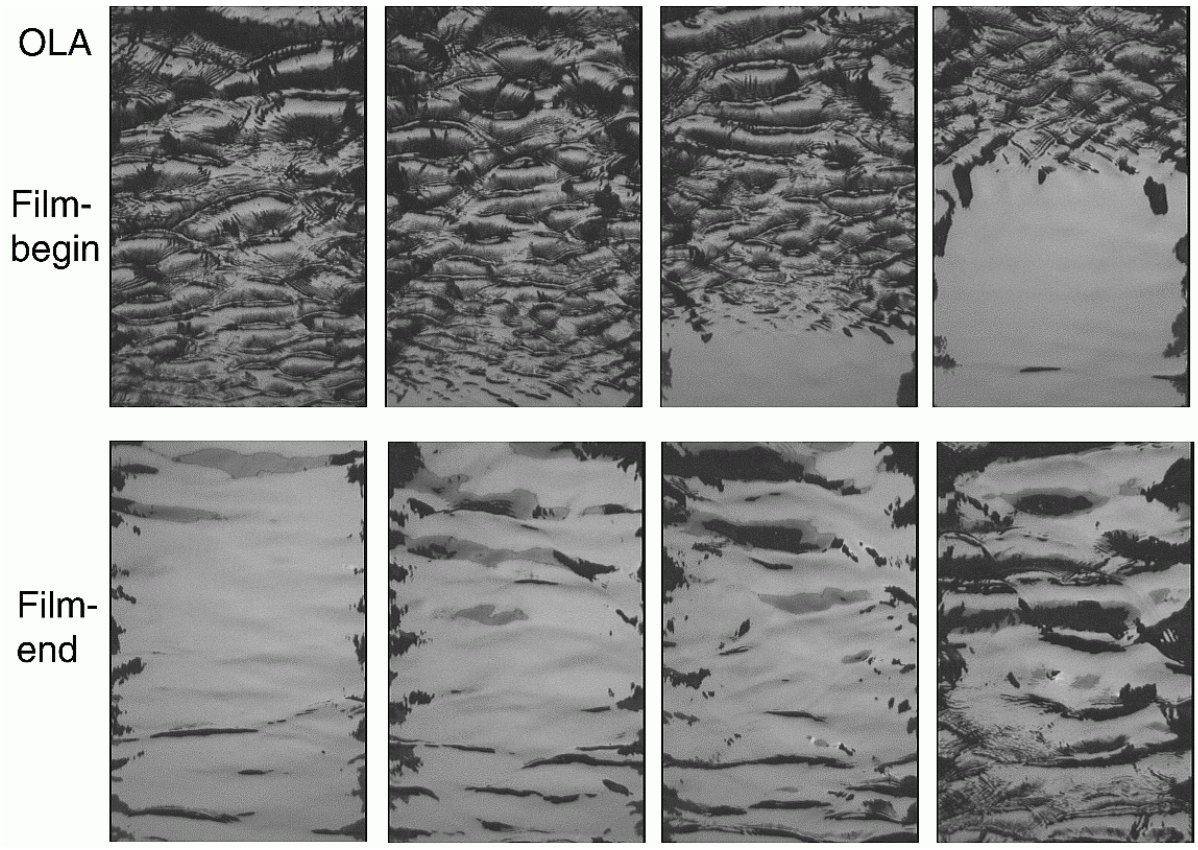

Fig. 10: series of video images taken while a slick consisiting of oleyl alcohol (abbreviated as OLA) was arriving at the camera's field-of-view. Note that the slick's forward edge is sharp, while its backward edge is diffuse and tattered.

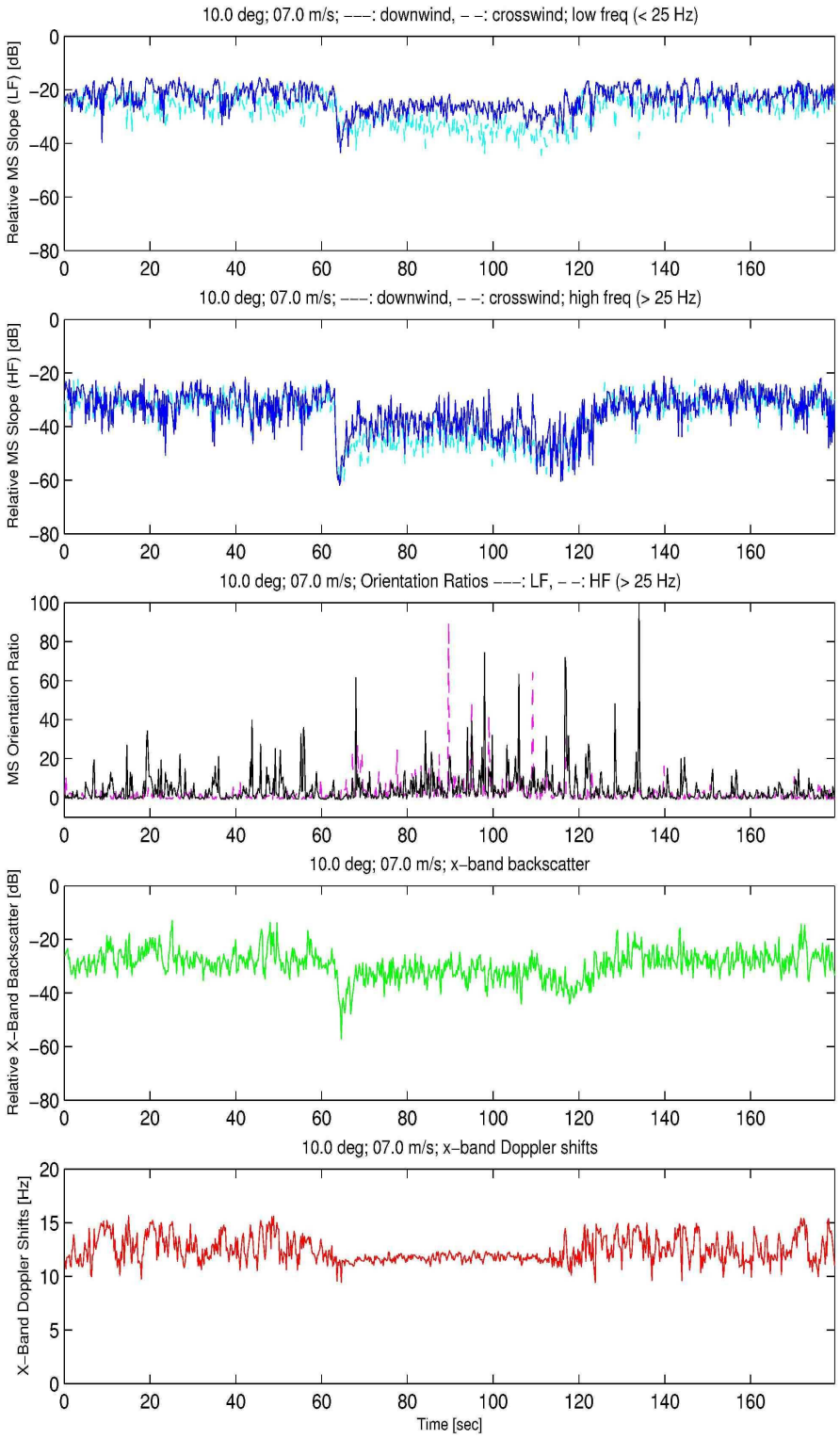

Fig. 11: results from measurements with a small slick consiting of palmitic acid methyl ester. From top to bottom: 1: downwind and crosswind slope (long-frequency part, f ≤ 25 Hz); 2: high-frequency downwind and crosswind wave slope (f > 25 Hz); 3: normalized orientation ratio, derived from downwind and crosswind wave slopes; 4: relative radar backscatter at X band; 5: radar Doppler shift at X band.

Measurements with a high-resolution W-band radar (Schlick et al., 2002; Gade et al., unpubl.)

W-band backscatter experiments have been performed at the wind-wave tank of the University of Hamburg using a coherent 94 GHz FMCW radar. The aim of the experiments was to study the backscatter mechanisms under shallow incidence angles and to compare the results with previous ones obtained with an X-band scatterometer. The measurements were performed at three grazing angles, 7.5°, 10°, and 20°, and at VV-, HH-, and VH-polarization. The wind speed ranged from 2 m/s to 10 m/s and was increased in steps of 1 m/s. The analysis of the acquired radar Doppler spectra showed that Bragg scattering from both bound and freely propagating Bragg waves is the dominant backscattering mechanism at all deployed wind speeds. In particular, at low wind speeds (up to 4 m/s), when the overall backscatter is small, bound waves are the dominating scatterers, whereas at higher wind speeds (5 m/s and above) the acquired signal is mainly caused by freely propagating Bragg waves. This is in qualitative agreement with similar findings that were made earlier with the X-band scatterometer working at moderate incidence angles.

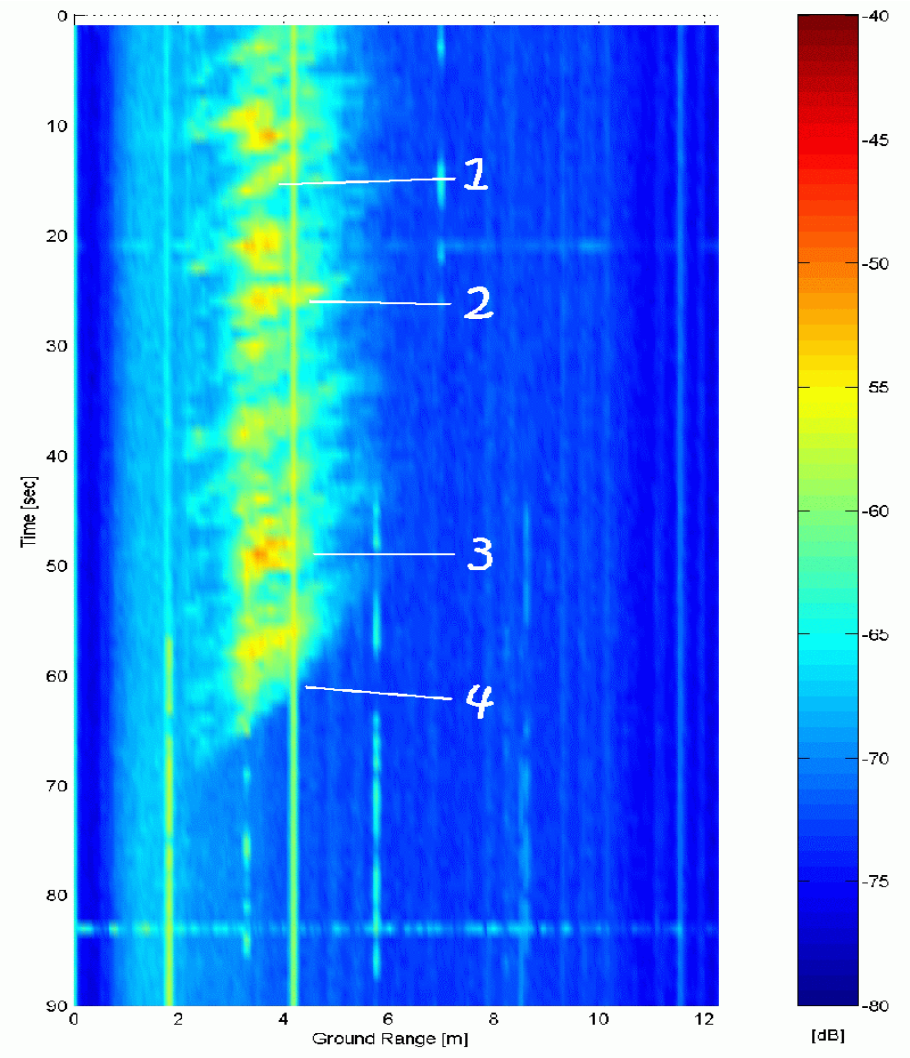

Fig. 12: 2-dimensional plot of the backscattered radar power at W band as a function of ground range and time. (1)-(3) denote detected features traveling at different speeds. During the measurement, a small slick consisting of palmitic acid methyl ester was drifting into the radar footprint causing an abrupt decrease of backscattered radar power (4).

More recently, we have performed wind-wave tank measurements at wind speeds between 2 m/s and 12 m/s and when small patches of monomolecular surface films were drifting through the footprint of the W-band radar. The aim of the experiments was to gain further insight into small-scale energy fluxes on the water surface and into the role surfactants may play in this frame. We measured the radar backscattering using an upwind-looking scatterometer working at 10 GHz (X band) and an upwind-looking radar working at 94 GHz (W band, range resolution: 5 cm) and the surface slope in the center of both radar footprints using a narrow-beam laser slope gauge. The measurements were performed at slick-free water surfaces and in the presence of small patches of surfactant palmitic acid methyl ester. While the slick patches were drifting through the measurement area, we observed a strong decrease in the mean wave slope and in the radar backscattering. This decrease is maximum at the slick's forward edge, because of its locally changed visco-elastic properties. Wave breaking events outside the slick patches could be identified from the X-band backscatter time series and from two-dimensional W-band backscatter maps. Our results will help to better understand the small-scale processes on the water surface, particularly at the crests of breaking waves.

References:

Alpers, W., and H. Hühnerfuss, 1989: The damping of ocean waves by surface films: a new look at an old problem, *J. Geophys. Res., 94,* 6251–6265.

Braun, N., M. Gade, and P.A. Lange, 1998: Laboratory measurements of artificial rain impinging on a water surface, *Proceed. Oceans'98,* IEEE, Piscataway, NJ, USA, 1817-1822.

Braun, N., M. Gade, and P.A. Lange, 1999a: Laboratory measurements of artificial rain impinging on a water surface, in *Operational Remote Sensing for Sustainable Development, G.A.Nieuwenhuis, R.A. Vaughan, M. Molenaar (eds.),* Balkema, Rotterdam, 339-344.

Braun, N., M. Gade, and P.A. Lange, 1999b: Radar backscattering measurements of artificial rain impinging on a water surface at different wind speeds, Proceed. Intern. Geosci. Remote Sens. Sympos. (IGARSS) '99, IEEE, Piscataway, NJ, USA, 200-202.

Braun, N., M. Gade, and P.A. Lange, 2002: The effect of artificial rain on wave spectra and multi-polarisation X band radar backscatter, *Int. J. Remote Sens., 23,* 4305-4322.

Feindt, F., 1985: Radar-Rückstreuexperimente am Wind-Wellen-Kanal bei sauberer und filmbedeckter Wasseroberfläche im X band (9.8 GHz), Dissertation, Fachbereich 15 (Geowissenschaften), Univ. Hamburg, Hamburg, Germany, 224 pp.

Gade, M., 1992: Untersuchungen zur Wellendämpfung von monomolekularen Oberflächenfilmen mit Hilfe von Wellendraht-, Laser- und Radarsonden, Diplomarbeit, Univ. Hamburg, FB Physik.

Gade, M., 1996: Untersuchungen zur Abbildung biogener und anthropogener Oberflächenfilme auf dem Meer mit Hilfe von Radarsensoren, Dissertation, Univ. Hamburg; Shaker Verlag, Aachen, 176 pp.

Gade, M., W. Alpers, H. Hühnerfuss, and P.A. Lange, 1998a: Wind-wave tank measurements of wave damping and radar cross sections in the presence of monomolecular surface films, *J. Geophys. Res., 103,* 3167-3178.

Gade, M., W. Alpers, S.A. Ermakov, H. Hühnerfuss, and P.A. Lange, 1998b: Wind-wave tank measurements of bound and freely propagating short gravity-capillary waves, *J. Geophys. Res.,* 103, 21697-21710.

Gade, M., N. Braun, and P.A. Lange, 1998c: Laboratory measurements of artificial rain impinging on a wind-roughened water surface, *Proceed. Intern. Geosci. Remote Sens. Sympos. (IGARSS) '98,* IEEE, Piscataway, NJ, USA, 2559-2561.

Gade, M., N. Braun, and P.A. Lange, 1998d: Laboratory measurements of artificial rain impinging on slick-free and slick-covered water surfaces, *Proceed. Oceans'98,* IEEE, Piscataway, NJ, USA, 1439-1444.

Gade, M., and P.A. Lange, 2001: On the Distribution of Small-Scale Roughness at the Edges of Monomolecular Surface Films, *Proceed. Oceans'01,* IEEE, Piscataway, NJ, USA, 2425-2431.

Gade, M., P.A. Lange, and H. Hühnerfuss, 2002: Remotely Sensing Bound and Free Small-scale Waves at the Edges of Monomolecular Surface Films in a Wind-wave Tank, *Proceed. Intern. Geosci. Remote Sens. Sympos. (IGARSS) '02,* IEEE, Piscataway, NJ, USA, 1108-1110.

Gade, M., 2002: Fernerkundungs-Experimente am Windwellenkanal der Universität Hamburg, DGM-Mitteilungen 2-3/2002, 26-30.

Hühnerfuss, H., 1986: The molecular structure of the system water/monomolecular surface film and its influence on water wave damping, Habilitation, Univ. Hamburg, Hamburg, Germany, 245 pp.

Hühnerfuss, H., P.A. Lange, J. Teichert, and H. Vollmers, 1976: A wind wave tunnel for the investigation of artificial slick wave damping and drift, *Meer. Mar. Tec., 7,* 23-26.

Hühnerfuss, H., P.A. Lange, and W. Walter, 1982: Wave damping by monomolecular surface films and their chemical structure. Part I: Variation of the hydrophobic part of carboxylic acid esters, *J. Mar. Res., 40,* 209–225.

Lange, P.A. and H. Hühnerfuss, 1978: Drift response of monomolecular slicks to wave and wind action, *J. Phys. Oceanogr., 8,* 142–150, 1978.

Lange, P.A., B.Jähne, J. Tschiersch, and I. Ilmberger, 1982: Comparison between an amplitude measuring wire and a slope-measuring laser water wave gauge, *Rev. Sci. Instrum.,* 651-655.

Lange, P.A. and H. Hühnerfuss, 1984: Horizontal surface tension gradients induced in monolayers by gravity water wave action, *J. Phys. Oceanogr., 14,* 1620–1628.

Lange, P.A., G. van der Graaf and, M. Gade, 2000: Rain-Induced Subsurface Turbulence Measured Using Image Processing Methods, *Proceed. Intern. Geosci. Remote Sens. Sympos. (IGARSS) '00,* IEEE, Piscataway, NJ, USA, 3175-3177.

Lobemeier, P., 1981: Wire probe for measuring high frequency sea waves, *J. Fluid Mech., 16,* 138-159.

Schlick, T., M. Gade, H.-H. Essen, K.-W. Gurgel, P.A. Lange, 2002: W-band Radar Backscattering at Low Grazing Angles Measured in a Wave Tank at Various Wind Speeds, *Proceed. Intern. Geosci. Remote Sens. Sympos. (IGARSS) '02,* IEEE, Piscataway, NJ, USA, 1825-1827.